Diaelastic effect of self-interstitials in Fe

B. Igarashi
Physics Department and Materials Research Laboratory, University of Illinois at Urbana-Champaign, Urbana, Illinois 61801

E. C. Johnson
The Aerospace Corporation, M2/248, P.O. Box 92957, Los Angeles, California 90009

A. V. Granato
Physics Department and Materials Research Laboratory, University of Illinois at Urbana-Champaign, Urbana, Illinois 61801
(Received 21 September 1992; revised manuscript received 8 April 1993)

Ultrasound is used to study the production and annealing of the diaelastic effect in Fe. Frenkel pairs created by 2.3-MeV-electron bombardment cause the shear moduli, C' and C_{44}, to soften by $(-27\pm2)\%$ and $(-17\pm4)\%$, per at. % pair, if resistivity per at. % pair is 20 $\mu\Omega$ cm. Smaller diaelastic effects were expected theoretically, given the high migration energy of self-interstitials in Fe. The magnitudes are of the same order as for Cu, but the observed anisotropy matches that detected in Mo, the only other bcc metal tested.

I. INTRODUCTION

Few measurements of the diaelastic-shear-modulus softening exist. Measurements in fcc Cu and Al have proven fruitful, though; for example, in helping to establish the ⟨100⟩-dumbbell configuration of self-interstitial atoms (SIA's) in fcc metals.[1] More recently, such measurements were key to a model of liquid and amorphous states of fcc metals.[2] The model applies to other systems as well, but the only other available diaelastic measurements are for bcc Mo, for which values given by two different sources differ substantially. Aside from their relevance to the above model, measurements in Fe are important for comparison with theoretical calculations for the configuration of self-interstitials of iron.

The diaelastic effect is a softening of shear moduli produced by the reaction of interstitial defects to shear stress. Near an interstitial the lattice is highly compressed, and a pair of neighboring atoms is susceptible to being tilted by shear stress: traverse restoring forces on the pair are negative, due to high repulsion between the pair.[3] In turn, the axial repulsive forces acting at a tilted angle apply a shear stress on the crystal.[4] Thus, in analogy with diamagnetism, an external stress field induces an additional stress field in the crystal. Similar to the distinctions between diamagnetism and paramagnetism, diaelasticity is independent of the temperature and frequency of applied stress.[5,6] in contrast to paraelasticity (anelastic relaxation), which depends on both.

An aspect unaddressed until recently is that this tilting of pairs of atoms may produce displacements along close-packed directions that extend well beyond the immediate locality of the defect. This leads to an unusually large entropy per defect, thus making SIA's plausible sources of liquid and amorphous states.[2] In fact, SIA's give rise to three universally known characteristics of amorphous materials:[7] (1) crystallographically equivalent configurations that provide multiple wells (often referred to as two-level tunneling systems, (2) low-frequency vibrational resonance modes; and (3) softening of shear moduli.

The limited available data,[1,8–11] including results of the present work, are listed in Table I. In the table the bulk modulus is $B=(C_{11}+2C_{12})/3$ and the shear moduli are C_{44} and $C'=(C_{11}-C_{12})/2$, in terms of the cubic elastic constants. The diaelastic effect is expressed as $d(\ln C)/dc$, the relative softening of the modulus per unit concentration of Frenkel pairs (FP's). The concentration of interstitials, c, was determined from resistivity measurements using $\rho_{FP}=2.5$, 4, 14, and 20 $\mu\Omega$ cm/at.% FP's for Cu, Al, Mo, and Fe, respectively. Cu is the only material for which a complete set of measurements is available. The results for Al and Mo given by Robrock were obtained using the same electron radiation source. The values for Mo are substantially smaller than those given by Okuda and Mizubayashi for fast neutron damage.

The diaelastic effect is a relatively strong effect. The softenings of shear moduli are an order of magnitude bigger than other effects of the self-interstitials, like relaxation volume and change of the bulk modulus, which are of the same order as the concentration of defects. In the case of fcc metals, the large diaelastic effect, together with its anisotropy, provides strong evidence that the in-

TABLE I. Diaelastic softenings from self-interestitials in Cu, Al, Mo, and Fe.

	$\frac{\partial \ln B}{\partial c}$	$\frac{\partial \ln C_{44}}{\partial c}$	$\frac{\partial \ln C'}{\partial c}$	Reference
Cu	2±2	−28±5	−13±3	1,8
Al		−27±2	−16±2	9
Mo		−5.5±2	−14±2	10
		−14	−28	11
Fe		−17±4	−27±2	Present work

terstitials are split, since the dumbbell atoms are highly compressed and expected to have large negative transverse spring constants, giving big diaelastic effects.[1,3]

The diaelastic effect is chosen to be measured in Fe because, first, it is the only material, besides Cu, for which there are numerical predictions of the diaelastic effect;[12] second, there are experimental advantages associated with the study of Fe because the migration energy for interstitials is high. Experiments can be conducted at higher irradiation temperatures and fluxes, resulting in significant savings of cost and time. The high migration energy in Fe is the highest known for fcc and bcc materials.

Interstitials in Fe have a migration energy of 0.3 eV,[13] as compared to 0.083 eV in Mo,[14] 0.115 eV in Al,[6] and 0.117 eV in Cu.[6] Interstitials in Fe do not anneal out until relatively high temperatures, near 100 K. Most recovery (80–85 %) is due to annihilation of interstitials and occurs during stage-I annealing. Substages I_A through I_D reflect annihilation of interstitials by their associated vacancies, and substage I_E (120–145 K) marks recombination between uncorrelated FP's, the temperature of the substage depending upon the distance separating the pairs. The last substage is suppressed if there is a high concentration of impurities that trap migrating interstitials. All the temperatures of stage-I annealing in Fe are much higher than those, for instance, in Mo, where stage-I ends at 40 K. The high migration energy has been attributed to ferromagnetism of Fe.[15,16]

The configuration of the self-interstitial in Fe is not universally agreed to. The theoretical calculations of Johnson,[17] Schober,[12] Erginsoy, Vineyard, and Engler,[18] and Taji *et al.*[19] concur with a ⟨110⟩-split configuration of the interstitial in Fe. Experimental evidence for this configuration is provided by internal friction measurements of Hivert *et al.*,[20] from magnetic relaxation measurements by Chambron, Verdone, and Moser[21] and from Huang x-ray scattering by Ehrhart.[22] However, magnetic after-effect results of Hirscher *et al.*[23] and internal friction measurements of Wolf and Kronmüller[24] indicate that this stage I_E interstitial has a ⟨111⟩-oriented configuration.

Predictions of the diaelastic effect are available only for the ⟨110⟩-split configuration and not the ⟨111⟩-oriented configuration. Librational resonance modes of the dumbbell give rise to the diaelastic effect, and diaelastic softenings are proportional to inverse squares of the resonant frequencies.[25] The ⟨110⟩ dumbbell gives two librational resonance modes, B_{1g} and B_{2g}, corresponding to dumbbell rotation in mutually perpendicular planes. Since resonant frequency, ω_{1g}, is less than ω_{2g}, and C' stress couples better than C_{44} does with the B_{1g} mode, Ram[26] expects C' softening to be bigger than C_{44} softening. Measurements in Mo bear out these expectations (see Table I). Ehrhart, Robrock, and Schober[6] similarly predict this result for bcc metals with low migration temperatures but expect diaelastic effects to be less in Fe due to its high migration temperature. Interstitial migration is thought to be driven by the librational resonance modes[3,27] and a high migration energy is taken to indicate that dumbbell tilting is reduced. Schober's[12] calculated results for the total softenings per FP, where the interstitial and vacancy are well separated, are nearly isotropic and much smaller than fcc diaelastic effects.

$$\frac{\partial \ln C_{44}}{\partial c} = -7.2(-0.3), \quad \frac{\partial \ln C'}{\partial c} = -6.2(-2.8) .$$

These figures include volume effects (see comments in discussion), and estimated image volume effects are indicated in parentheses. One attributes the smaller dumbbell tilting to a strengthening of transverse spring constants by the dumbbell's effect on local ferromagnetism.[16]

II. EXPERIMENTAL TECHNIQUE

Ultrasonics measurements are performed on single crystals of α iron cut from two boules of Armco Fe (Monocrystals Co. of Cleveland, OH). Secondary ion mass spectroscopy (SIMS) analysis performed on boule No. 1 indicates that concentrations of C (577 at. ppm), N (207 at. ppm), and O (3735 at. ppm) match typical levels of Armco Fe. Other expected impurities are S (400 at. ppm), Mn (200 at. ppm), Si (trace), and P (90 at. ppm).[28,29] Most of the interstitial impurities are expected to be in the form of precipitates, though; the solubility limit of interstitial impurities in solid solution is approximately 1000 ppm [C (300 at. ppm), N (40 at. ppm), O (300 at. ppm), and S (300 at. ppm)].[30] Thin foil resistivity samples are cut from both boules and the resistivity ratios are 21. If room-temperature resistivity is 11 ± 1 $\mu\Omega$ cm,[29,31] resistivity of all interstitial impurities is close to that for C or N, 6.5 $\mu\Omega$ cm/at.%,[32] and interstitial impurities in solid solution dominate the residual resistivity; then the resistivity ratio indicates that the concentration of interstitial impurities in solid solution is indeed near 1000 ppm.

Each cylindrical bulk sample (roughly 7 mm long) is hand lapped on granite blocks to produce a pair of ⟨110⟩ faces parallel to within 70 sec of arc. A quartz transducer is mounted with Nonaq stopcock grease to give shear waves in either the C' or C_{44} mode. Resonant frequency and attenuation are monitored with a pulse-echo superposition system described in detail by Read and Holder.[33] Changes in resonant frequency f are related to changes in the elastic constant C and the volume V by the relation,

$$\frac{\Delta C}{C} = \frac{2\Delta f}{f} - \frac{\Delta V}{3V} \approx \frac{2\Delta f}{f} .$$

Changes of the resonant frequency are resolvable on the order of one part in 10^7.

Bulk samples are potted in a brass holder with indium and placed in a closed-cycle refrigerator-cryostat system designed by Johnson.[34] The apparatus permits irradiation by 2.3-MeV electrons from a Van de Graaf accelerator and *in situ* ultrasonic measurements. The rate of FP production is calibrated by resistivity changes in the thin foil sample mounted in front of the bulk sample (assumes $\rho_{FP}=20$ $\mu\Omega$ cm/at.% FP).[6,35,36]

Table II lists the parameters for the experiments. In trial 1, 10- and 30-MHz data are extracted simultaneously. In trials 6 and 7, a pair of ceramic cobalt magnets are attached to the sample holder to magnetize the sample in

TABLE II. Elastic modulus measured, resonant ultrasonic frequency, maximum temperature of irradiation, specimen boule, and whether resistivity is measured or magnetic field is applied.

Trial	Elastic modulus	Frequency (MHz)	Irradiation temperature (K)	Sample No.	Resistivity measured?	Magnetic field?
1	C_{44}	11.10 &28.61	50	1	no	no
2	C'	27.48	45	1	yes	no
3	C'	10.86	45	1	yes	no
4	C'	10.86	23	1	yes	no
5	C'	11.45	45	1	no	no
6	C'	10.97	58	2	no	yes
7	C'	9.94	51	2	yes	yes

the easy ⟨100⟩ direction. The strength of the field in trial 7 is at least 0.1 T, sufficient to freeze magnetic domain (Bloch) walls, as shown at room temperature by cancellation of the ΔE effect. The ΔE effect is a softening of the Youngs modulus resulting from Bloch wall motion,[37] and, in Fe, the ⟨100⟩ Youngs modulus and, therefore, the C' shear modulus are susceptible to this effect. The strength of the field in trail 6 is weaker, and Bloch walls may not be frozen entirely.

A sample is irradiated briefly and the temperature is raised well above stage-I annealing to pin any loose dislocations with SIA's or impurity-SIA complexes, although dislocations probably are well pinned already by impurities. During the main irradiation, after each session, velocity, and attenuation are measured between 4.2 and ~20 K, and, if a resistivity sample is mounted, resistance is measured at 4.2 K. After the final irradiation session, FP's are annealed isochromally at 1 K/min to a given temperature, annealed isothermally for ten min, and ramped down at 1 K/min. Successive isothermal anneals are spaced apart 15 or 20 K. Between trials 2 and 3 the temperature is not raised above 200 K. Due to constraints of the ultrasonic bond, data cannot be taken above 190 K.

III. EXPERIMENTAL RESULTS

Shear moduli steadily drop as irradiation damage accumulates. The drop cannot be due to a relaxation because no attenuation peak is evident (particularly below 20 K). Also, the drop is generally independent of temperature, as illustrated by 30 MHz measurements of C_{44} [Fig. 1(a)]. However, for the 10 MHz measurements of C_{44} and C' trials 2, 3, and 7, a small peak extending between 6 and 15 K of unknown origin (possibly a magnetoelastic effect) is noted. If measurements are taken away from this interference, then the shear moduli drop linearly with FP production, and comparison against 30-MHz data shows the drops are independent of frequency [Figs. 1(b) and 1(c)], contrary to expectations for a relaxation, but consistent with a diaelastic effect. For C', the slope of the 30-MHz data appears a little larger than that of 10 MHz, but the discrepancy is likely due to error in the damage rate of the 30-MHz trial; unlike the C_{44} measurements, 30- and 10-MHz data are not taken concurrently. To accommodate different damage rates, data points are plotted in Fig. 1(c) as functions of estimated damage instead of raw counts of irradiation. Data of trial 4 is available only at 4.2 K, unfortunately, where error for this trial is relatively high, possibly due to the above-mentioned interference. Data points for the C_{44} trials are adjusted slightly to compensate for a brief accidental anneal after the first irradiation session. In all graphs, error bars that are not much bigger than data points are omitted.

Calculations of the diaelastic effects are listed in Table III. Slopes of weighted linear fits to diaelastic softenings per count of irradiation are divided by estimates of rates of FP production to give $\partial \ln C_{44}/\partial c$ or $\partial \ln C'/\partial c$, the diaelastic relative softenings per unit FP concentration.

TABLE III. Slopes of diaelastic softenings per count of irradiation, estimates of rates of FP generation, and diaelastic effects as relative softenings per unit FP concentration. Frenkel pair resistivity is assumed to be 20 $\mu\Omega$ cm/at.% FP.

Trial	Elastic modulus	$10^6 \frac{\Delta C}{C}$ / 1000 counts	at ppm FP / 1000 counts	$\frac{\partial \ln C}{\partial c}$
1	C_{44}	−6.44 (±0.14)	0.370 (±0.81)	−17.4 (±3.8)
2	C'	−8.16 (±0.21)	0.272 (±0.049)	−30.0 (±5.4)
3	C'	−6.10 (±0.16)	0.223 (±0.024)	−27.4 (±3.0)
4	C'	−7.65 (±0.60)	0.286 (±0.029)	−26.7 (±3.5)
7	C'	−2.89 (±0.055)	0.133 (±0.015)	−21.7 (±2.4)

The C_{44} slope is the average of the 30- and 10-MHz slopes. Since no resistivity measurements are conducted during this mode, the damage rate is extrapolated from damage rates of unmagnetized C' trials, with 22% uncertainty. The higher damage rate reflects the absence of shielding by a resistivity sample. The final diaelastic effect is $\partial \ln C_{44}/\partial c = -17 \pm 4$. C' trials conducted without resistivity measurements (trials 5 and 6) are omitted from Table III. The best estimate of the unmagnetized C' diaelastic effect is the weighted average of the values of trails 3 and 4, $\partial \ln C'/\partial c = -27 \pm 2$ [line with intermediate slope in Fig. 1(c)], a bigger effect than the magnetized C' diaelastic effect, -22 ± 2 (line with shallower slope). These calculations of the diaelastic effects scale with the FP resistivity, ρ_{FP}, assumed to be 20 $\mu\Omega$ cm/at.% FP. If ρ_{FP} is 30 $\mu\Omega$ cm/at.% FP,[38] then $\partial \ln C'/\partial c = -41$ and $\partial \ln C_{44}/\partial c = -26$; if ρ_{FP} is 12.5 $\mu\Omega$ cm/at.% FP,[39] then $\partial \ln C'/\partial c = -17$ and $\partial \ln C_{44}/\partial c = -11$.

Annealing results are shown in Fig. 2. Resistivity recovery is shown in Fig. 2(a), and the curves agree within estimated error, except near 80 K, where trial 4 better reproduces previous studies.[39,40] Anneals of all 10-MHz C' trials are shown in Figs. 2(b) and 2(c). The unmagnetized C' trials display a curious overhardening that grows from 90 to 120 K (in trial 4, overhardening starts at 75 K). Overhardenings in trials 3, 4, and 5 are $\Delta C'/C' \approx 10^{-4}$, although three successive anneals at 120 K (with the third isothermal anneal lasting an hour) are required to reach this magnitude during trial 5. [In Fig. 2(c), the recoveries are plotted relative to the respective diaelastic effects of the various trials, and the overhardenings appear different among all trials.] Results of trials 6 and 7 demonstrate that the overhardening diminishes with increasing applied magnetic field. There is evidence that C_{44} overhardens during annealing, too. Figure 2(d) shows that the rate of C_{44} recovery for 120–160 K exceeds rates of recoveries of resistivity and magnetized

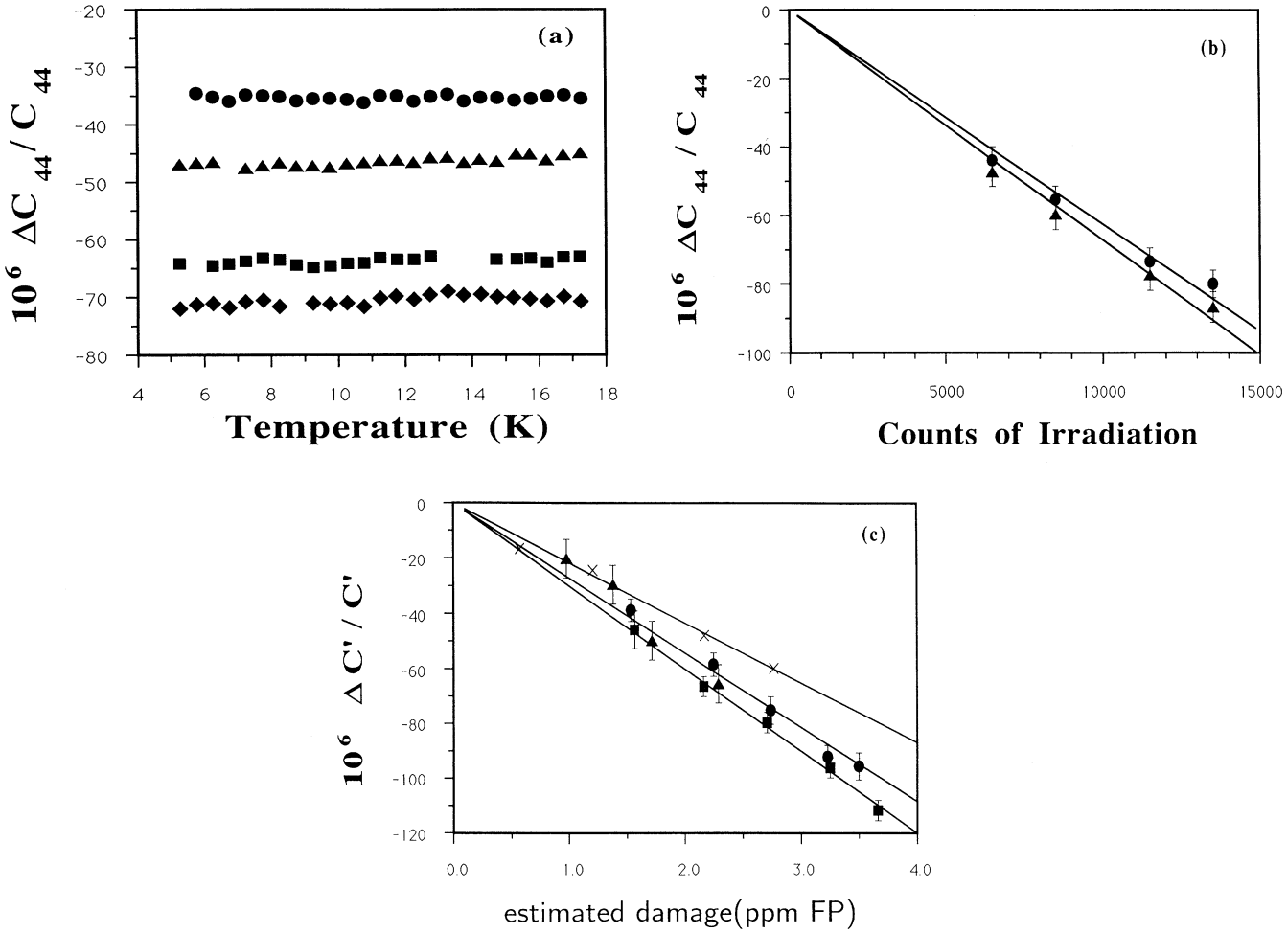

FIG. 1. (a) C_{44} (28.61 MHz) softenings vs temperature. (●) after 6500 counts. (▲) after 8500 counts. (■) after 11 500 counts. (◆) after 13 500 counts. (b) C_{44} diaelastic shifts vs counts of irradiation. (●) 28.61 MHz measurements. (▲) 11.10 MHz measurements. (c) C' diaelastic shifts vs counts of irradiation. (●) 10.86 MHz (trial 3). (▲) 10.86 MHz (trial 4). (■) 27.48 MHz (trial 2). (×) 9.94 MHz, magnetized (trial 7). For the last trial, error bars are not much bigger than data points.

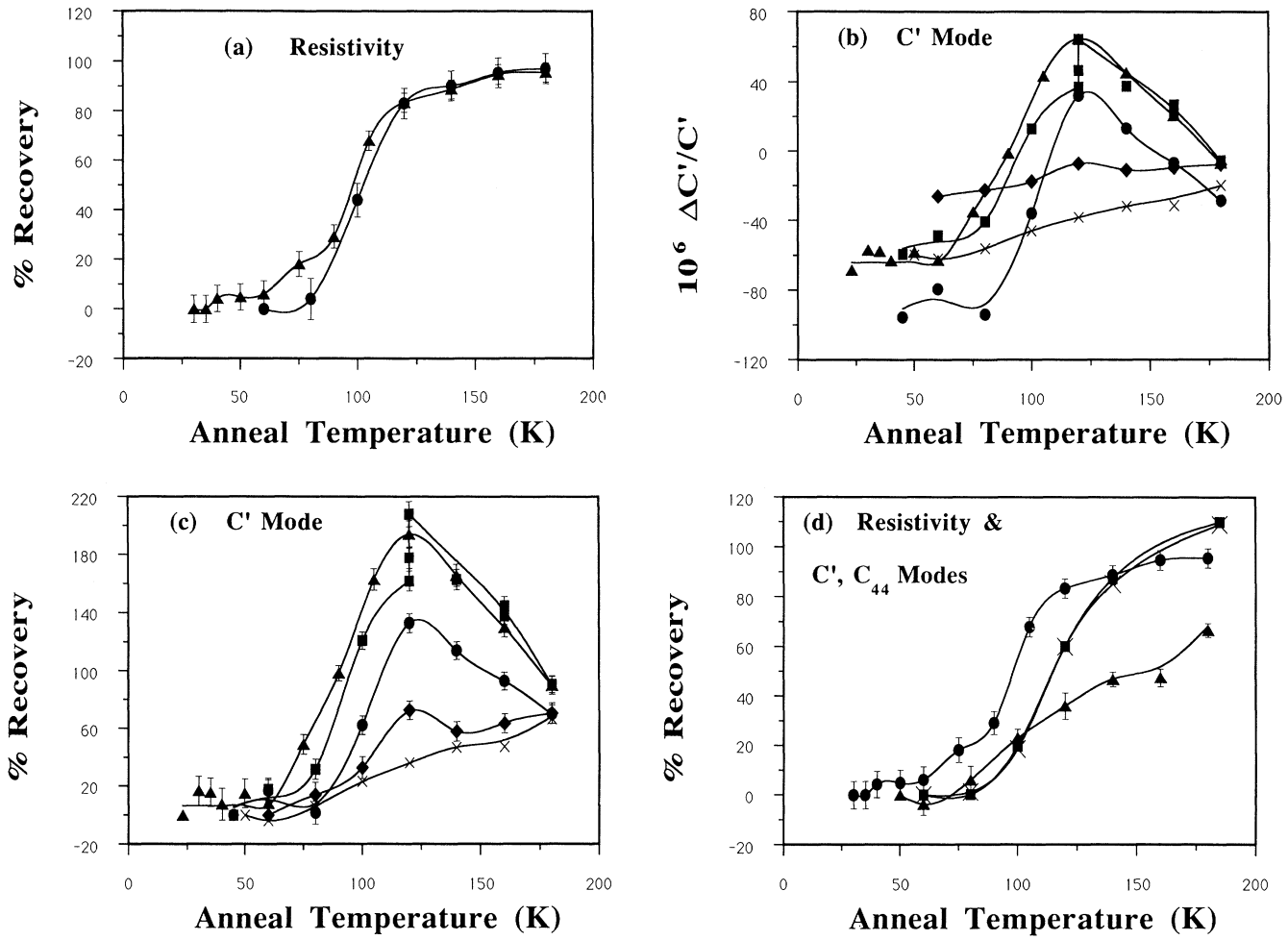

FIG. 2. (a) Resistivity recoveries as a function of temperature of isothermal anneal. (●) trial 3. (▲) trial 4. (b) and (c) Annealings of C' diaelastic effect. (●) trial 3. (▲) trial 4. (■) trial 5. (◆) trial 6, magnetized. (×) trial 7, magnetized. (d) Annealings of resistivity and C' and C_{44} diaelastic effects. (●) resistivity (trial 4). (▲) C', magnetized (trial 7). (■) C_{44}, 28.61 MHz (trial 1). (×) C_{44}, 11.10 MHz (trial 1). Error bars that are not much bigger than data points are omitted.

C', and by 140 K the C_{44} and C' softenings probably are too anisotropic to be explained on the basis of the diaelastic effect alone. Unlike the C' case, the C_{44} overhardening persists through higher temperature anneals, and by 185 K recovery exceeds 100%.

IV. DISCUSSION

The moduli softenings per FP are taken to reflect mostly the diaelastic effect of the interstitial. Vacancies do not give rise to high compression of nearest neighbors, as is expected with interstitials. Schober calculates the relative softenings per unit concentration of vacancies to be smaller than -5, similar to results for vacancies in copper.[3,12] Volume effect corrections are likewise small. Softenings due to local ($\delta\nu^{\infty}$) and image ($\delta\nu^{\mathrm{im}}$) volumes in the FP are[41]

$$-\frac{1}{3}\frac{\delta\nu^{\infty}}{\Omega}-\frac{\delta\nu^{\mathrm{im}}}{\Omega}\frac{B}{C}\left[\frac{\partial C}{\partial P}\right]_T$$

where Ω is the atomic volume, B the modulus, and C is the appropriate shear modulus. The local volume change does not affect nearest-neighbor separations at sites away from the defects and the first term is the softening from expansion of a harmonic crystal. Conversely, the image volume is uniform expansion of the crystal, and the second term contains both harmonic and anharmonic effects of the expansion.[42] An approximation for these volume effects may be obtained by using measurements of elastic constants at 4 K ($C_{44}=1.219\times10^{12}$ dyn/cm^2), $C'=0.525\times10^{12}$ dyn/cm^2, $B=17.31\times10^{12}$ dyn/cm^2),[43] a continuum approximation for the image volume ($\delta\nu^{\mathrm{im}}=0.69\delta\nu^{\infty}$ in Fe), and measurements of pressure derivatives of the elastic constants at room temperature ($\partial C_{44}/\partial P=2.63$, $\partial C'/\partial P=1.11$).[44] For both C' and C_{44}, softenings per unit FP concentration from volume effects are approximately

$$\frac{\delta C}{cC}=-2.9\frac{\delta\nu^{\infty}}{\Omega}=-1.7\frac{\delta\nu^{\mathrm{relax}}}{\Omega}\cong-1.8$$

where δv^{relax} is the total volume change per FP, 1.05 Ω.[6,36] Thus, volume effects account for only small fractions of the observed softenings.

The potential influences of internal stress from vacancies and impurities and of magnetostriction strain are recognized, but hard to predict quantitatively. In close pair FP's, stress from the vacancy affects compression of atoms about the interstitial, but it depends on orientation of the axis separating the pair: the bcc lattice is compressed along ⟨100⟩-type directions away from the vacancy, but stretched in other directions.[45] Thus, the influence of vacancies is mixed (as is true for impurities, although, on average, vacancies should relieve compression of atoms about the interstitial and suppress the diaelastic effect. Magnetostriction distorts every domain, and a domain with its magnetization parallel to the ⟨100⟩ axis, for example, is spontaneously stretched along this axis 0.003%,[46] a bigger distortion than the ultrasonic shear strain. If SIA's are split interstitials, then the compression of ⟨110⟩ and ⟨101⟩ dumbbells is relieved, but ⟨011⟩ dumbbells may be compressed. Since more dumbbells are stretched than compressed, the likely net influence of magnetostriction is to lower the diaelastic effect. These reductions from vacancy stress and magnetostriction cannot be large, though; otherwise, it would imply that the diaelastic effects would be unrealistically high when vacancies or magnetostriction do not interfere. The effect of impurity stress likely is of similar scale as the effect of vacancy stress, and is small.

A potential parallel source of C' softening comes from disruption of ferromagnetic ordering by creation of interstitials. (The perturbation from vacancies is expected to be much less.) Ferromagnetism significantly strengthens C' by splitting spin degeneracy of the e_g band at the Fermi level and preventing the occurrence of a band Jahn-Teller effect that weakens second-nearest-neighbor spring constants in paramagnetic Fe.[47] If the interstitial is a ⟨110⟩ dumbbell, Ono estimates that the lattice is like a compressed fcc lattice and concludes that magnetization is lowered.[16] It is unknown how much the lattice resembles a compressed fcc lattice when the concentration of interstitials is low, as in this experiment, and whether ferromagnetic ordering is disturbed sufficiently for a band Jahn-Teller effect to occur. However, any C' softening subtracts from the measurements of the C' diaelastic effect and likely is limited, if the diaelastic effect is to have anisotropy predicted for the split interstitial, consistent with Ono's assumption of this configuration.

The lower C' diaelastic effect obtained when the sample is magnetized (trial 7) may be due to coupling between point defects and local magnetization. This coupling is described elsewhere in relation to the magnetic after effect,[48] where it is explained that a point defect adds a local magnetization anisotropy energy that establishes preferred alignments of moments on surrounding atoms. As a point defect moves, one might expect magnetization on surrounding atoms to rotate; conversely, if the magnetization direction is fixed by an external field, motion of the point defect should be constrained.

Since overhardening of C' during the anneals disappears when a sample is magnetized initially and domain walls are frozen, the hardening is attributed to wall motion; that is, to dampening of that motion. The C' modulus is softened by wall motion according to the ΔE effect, but if wall mobility decreases then the ΔE effect is partially suppressed and C' becomes relatively stiffer. Overhardening is observed to increase during stages $I_C - I_E$ (90–120 K), where, due to the high concentration of impurities in solid solution, SIA's likely are trapped [for example, by C (Refs. 40 and 49) and Mn (Ref. 50)]. (In trial 4, overhardening starts earlier at 75 K, and it may be due to SIA's being trapped by defect species leftover from trial 3.) Interstitial C atoms effectively increase wall viscosity, but viscosity from impurity-SIA complexes may be higher, thus accounting for the overhardening. Point defects raise wall viscosity if they are embedded in walls, where coupling with local magnetization impedes rotation of moments. Also, point defects affect walls through interaction between the defect internal stress and magnetostriction stress.[48]

SIA's alone might raise wall viscosity, too, but probably less than impurity complexes (particularly with interstitial impurities). (Also, Ono finds that FP's in Fe affect wall mobility less than in Ni.[16]) Increase of wall viscosity by SIA's during irradiation is expected to be small. If the effect of SIA's on walls were large, then hardening might be expected to grow nonlinearly, due to distribution of wall mobilities and pinning centers in the walls; however, only a linear net change of C' is observed during irradiation. Any hardening that occurs is less than hardening produced by a magnetic field, since net softening is still bigger than when the sample is magnetized (trial 7).

Decline of C' overhardening after I_E is taken to reflect migration or dissociation of the impurity-SIA complexes that interfere with wall motion. Previous studies suggest that Fe-Mn complexes migrate shortly before I_E (Ref. 50) and that the continuum of stage-II annealing may include agglomeration of Fe-C complexes at 146 K (Ref. 51) and dissociation at 160 K (Ref. 40). Similar to the diffusion after effect,[48] impurity-SIA complexes embedded in walls might undergo long-range diffusion, due to translational forces exerted by varying magnetic moments of the wall. Decrease of wall viscosity may result then from complexes either migrating out of the walls or becoming trapped by agglomerates or precipitates, with the result of reducing their dampening of wall motion.

C_{44} hardening similarly is attributed to suppression of the ΔE effect. In contrast to C' softening, C_{44} softening is derived from the ΔE effect of ⟨111⟩ tension, which in Fe results from rotation of magnetization of domains. Agglomeration or growth of precipitates may be responsible for the hardening, which only represents about 1% of the ΔE effect.[52] No hardening appears below stage I_E, since the smaller isolated point defects are not expected to inhibit rotation significantly.

V. CONCLUSIONS

The diaelastic effect of Fe is large, as in Cu. However, the anisotropy of the effect is reversed, as with the other bcc metal tested, Mo ($-\partial \ln C'/\partial c > -\partial \ln C_{44}/\partial c$). In

fact, the present results are close in magnitude to those of Okuda and Mizubayashi's results for neutron-irradiated Mo.

Sizes of the effects are in disagreement with expectations of Ehrhart, Robrock, and Schober[6] and the effects are both much larger and more anisotropic than Schober's results.[12] The reason for this discrepancy is unknown. Influences of wall viscosity from SIA's, stress from nearby vacancies, stress from nearby impurities, magnetostriction strain, and changes of ferromagnetism have not been estimated quantitatively, but the first, second, and fourth factors only serve to depress the measured diaelastic effect, and effects of the third and fifth factors likely are limited. Measurements conform with Ram's[26] predictions for a ⟨110⟩-split interstitial (and the predictions of Ehrhart *et al.* for bcc metals with low migration temperatures), with the anisotropy consistent with a resonant frequency ω_{1g} that is less than ω_{2g}.

Pending the calculation of diaelastic effects expected from the ⟨111⟩-oriented configuration, it remains uncertain whether these results are evidence in favor of the split configuration over the ⟨111⟩-oriented configuration. Extrapolating from explanations of the large diaelastic effects produced by split configurations, though, to account for the observed large diaelastic effects, it seems necessary that the modeling of the ⟨111⟩-oriented configuration would have to provide for low-frequency resonance modes that couple with shear stresses.

The trend among fcc and bcc metals tested so far is that the diaelastic effect is sizable. The softenings of shear moduli produced by self-interstitials are an order larger than those produced by vacancies. A large diaelastic effect is consistent with a model of phase transformations of fcc metals between condensed matter states that is based on changing populations of self-interstitials.[2] It seems likely that this model applies to bcc metals as well.

ACKNOWLEDGMENTS

This work was supported by the U.S. Department of Energy under Contract No. DE-AC02-76ER01198 and The Aerospace Corporation.

[1]J. Holder, A. V. Granato, and L. E. Rehn, Phys. Rev. Lett. **32**, 1054 (1974).

[2]A. V. Granato, Phys. Rev. Lett. **68**, 974 (1992).

[3]P. H. Dederichs, C. Lehmann, H. R. Schober, A. Scholz, and R. Zeller, J. Nucl. Mater. **69&70**, 176 (1978).

[4]For detailed discussion, see K. H. Robrock, *Mechanical Relaxation of Interstitials in Irradiated Metals,* Springer Tracts in Modern Physics, Vol. 118 (Springer, Berlin, 1990), p. 14

[5]P. Ehrhart, in *Atomic Defects in Metals,* Landolt-Börnstein Numerical Data and Functional Relationships in Science and Technology, New Series, Group III: Crystal and Solid State Physics, Vol. 25, edited by H. Ullmaier (Springer-Verlag, Berlin, 1991), p. 88.

[6]P. Ehrhart, K-H. Robrock, and H. R. Schober, in *Physics of Radiation Effects in Crystals,* Modern Problems in Condensed Matter Science, Vol. 13, edited by R. A. Johnson and A. N. Orlov (Elsevier, Amsterdam, 1986), p. 3.

[7]A. V. Granato, in *Phonon Scattering in Condensed Matter VII,* Proceedings of the Seventh International Conference, Cornell University, Ithaca, New York, 1992, edited by M. Meissner and R. O. Pohl, Springer Series in Solid State Sciences, Vol. 112 (Springer-Verlag, Berlin, 1993).

[8]L. E. Rehn, J. Holder, A. V. Granato, R. R. Coltman, and F. W. Young, Jr., Phys. Rev. B **10**, 349 (1974); J. Holder, A. V. Granato, and L. E. Rehn, *ibid.* **10**, 363 (1974).

[9]K-H. Robrock and W. Schilling, J. Phys. F **6**, 303 (1976).

[10](a) K-H. Robrock, in *Point Defects and Defect Interactions in Metals,* Proceedings of the Yamada Conference V, Kyoto, 1981, edited by J.-I. Takamura, M. Doyama, and M. Kititani (University of Tokyo Press, Tokyo, 1982), p. 179; (b) H. Jacques (unpublished), as cited in Ref. 6, p. 71.

[11]S. Okuda and H. Mizubayashi, in Ref. 10(a), p. 179.

[12]H. R. Schober, J. Nucl. Mater. **126**, 224 (1983).

[13]A migration energy of 0.27 eV is found by the resistivity study of S. Takaki, J. Fuss, H. Kluger, U. Dedek, and H. Schultz, Radiat. Effects **79**, 87 (1983); however, a migration energy of 0.32 eV is found by magnetic relaxation measurements of L. Verdone, W. Chambron, and P. Moser, Phys. Status Solidi B **61**, K41 (1974).

[14]H. Kluger, L. A. Schwirtlich, S. Takaki, U. Ziebart, and H. Schulz, in Ref. 10(a), p. 191.

[15]P. Lucasson, F. Maury, and A. Lucasson, *Proceedings of the International Conference on Vacancies and Interstitials in Metals and Alloys, Berlin, 1986* [Mater. Sci. Forum, **15-18**, 231 (1987)].

[16]F. Ono, H. Maeta, and J. P. Jakubovics, Physica B **161**, 186 (1989).

[17]R. A. Johnson, Phys. Rev. **134**, 1329 (1964).

[18]C. Erginsoy, G. H. Vineyard, and A. Engler, Phys. Rev. **133**, A595 (1964).

[19]Y. Taji, T. Iwata, T. Yokkota, and M. Fuse, Phys. Rev. B **39**, 6381 (1989).

[20]V. Hivert, R. Pinchon, H. Bilger, P. Bichon, J. Verdone, D. Dautreppe, and P. Moser. J. Phys. Chem. Solids **31**, 1854 (1970).

[21]W. Chambron, J. Verdone, and P. Moser, in *Proceedings of the International Conference on Fundamental Aspects of Radiation Damage in Metals, Gatlinburg, 1975,* edited by M. T. Robinson and F. W. Young, Jr., (U.S. Department of Commerce, Springfield, VA, 1976), p. 463.

[22]P. Ehrhart, in *Dimensional Stability and Mechanical Behavior of Irradiated Materials and Alloys* (British Nuclear Energy Society, London, 1983), Vol. 1, p. 101.

[23]M. Hischer, B. Schwendemann, W. Frank, and H. Kronmüller, in Ref. 15, p. 249.

[24]J. Wolf and H. Kronmüller, in Ref. 15, p. 255.

[25]P. H. Dederichs and R. Zeller, in *Point Defects in Metals II,* Springer Tracts in Modern Physics Vol. 87, edited by G. Höhler and E. A. Niehisch (Springer, Berlin, 1980), p. 139.

[26]P. N. Ram, Phys. Rev. B **43**, 6977 (1991).

[27]C. P. Flynn, Thin Solid Films **25**, 37 (1975).

[28]H. E. Hungerford, in *Reactor Handbook, Vol. 1: Materials,* 2nd ed., edited by C. R. Tipton (Interscience, New York, 1960), p. 1063; citing data from *Metals Handbook,* 1948 ed., edited by T. Lyman (American Society for Metals, Cleveland, 1948).

[29]*American Society of Mechanical Engineering Handbook, Vol. 2: Metals Properties,* 1st ed., edited by S. L. Hoyt (McGraw-Hill, New York, 1954), p. 4.
[30]R. M. Bozorth, *Ferromagnetism* (Van Nostrand, Toronto, 1951), p. 64.
[31]*Metals Handbook, Vol. 1: Properties and Selection of Metals,* 8th ed., edited by T. Lyman (American Society for Metals, Metals Park, 1961), p. 1209.
[32]H. Wagenblast and S. Arajs, Phys. Status Solidi **26**, 409 (1968); J. Appl. Phys. **39**, 5885 (1968).
[33]D. T. Read and J. Holder, Rev. Sci. Instrum. **43**, 933 (1972).
[34]E. C. Johnson, Rev. Sci. Instrum. **58**, 2295 (1987).
[35]R. Averbach (private communication). A comparable value of 19 $\mu\Omega$ cm/at. % FP's is obtained by A. Lucasson and R. M. Walker (unpublished) (cited in Ref. 39).
[36]P. Ehrhart, Mater. Res. Soc. Symp. **41**, 13 (1985).
[37]W. Döring, Z. Phys. **114**, 597 (1939).
[38]F. Maury, M. Biget, P. Vajda, A. Lucasson, and P. Lucasson, Phys. Rev. B **14**, 5303 (1976).
[39]P. G. Lucasson and R. M. Walker, Phys. Rev. **127**, 485 (1962).
[40]S. Takaki *et al.,* Ref. 13.
[41]P. H. Dederichs and C. Lehmann, Z. Phys. B **20**, 155 (1975).
[42]G. Liebried and N. Breuer, *Point Defects in Metals I: Introduction to the Theory,* Springer Tracts in Modern Physics Vol. 81 (Springer, Berlin, 1978), p. 279.
[43]J. A. Rayne and B. S. Chandrasekhar, Phys. Rev. **122**, 1714 (1961).
[44]Averages of values cited by C. A. Rotterand and C. S. Smith, J. Phys. Chem. Solids **27**, 267 (1966); and M. W. Guinan and D. N. Beshers, *ibid.* **29**, 541 (1968).
[45]F. Maury and P. Lucasson, Phys. Status Solidi A **34**, 513 (1976).
[46]S. Chikazumi, *Physics of Magnetism* (English edition prepared with assistance of S. Charap) (Wiley, New York, 1964).
[47]H. Hasegawa, M. W. Finnis, and D. G. Pettifor, J. Phys. F **17**, 2049 (1987).
[48]H. Kronmüller, in *Vacancies and Interstitials in Metals, Proceedings of the International Conference, Jülich, 1968,* edited by A. Seeger, D. Schumacher, W. Schilling, and J. Diehl (North-Holland, Amsterdam, 1970), p. 667.
[49]J. L. Leveque, T. Anagnostopoulos, H. Bilger, and P. Moser, Phys. Status Solidi **31**, K47 (1969).
[50]F. Maury, A. Lucasson, P. Lucasson, Y. Loreaux, and P. Moser, J. Phys. F **16**, 523 (1986).
[51]J. L. Leveque, T. Anagnostopoulos, H. Bilger, and P. Moser, Phys. Status Solidi **29**, K179 (1968).
[52]Formulas for the ΔE effects of Fe may be derived similar to those for the ΔE effects of Ni (Ref. 37). When volume magnetostriction is ignored, $\Delta C_{44}/C_{44} = -3C_{44}\lambda_{111}^2/K_1$, where λ_{111} is the magnetostriction constant along the $\langle 111 \rangle$ axis and K_1 is a parameter of the magnetic anisotropy energy.